

# Thermodynamic Geometric Control of Active Matter

Yating Wang,<sup>1</sup> Enmai Lei,<sup>1</sup> Yu-Han Ma,<sup>1</sup> Z. C. Tu,<sup>1,\*</sup> and Geng Li<sup>2,†</sup>

<sup>1</sup>*School of Physics and Astronomy, Beijing Normal University, Beijing 100875, China*

<sup>2</sup>*School of Systems Science, Beijing Normal University, Beijing 100875, China*

Active matter represents a class of non-equilibrium systems that constantly dissipate energy to produce directed motion. The thermodynamic control of active matter holds great potential for advancements in synthetic molecular motors, targeted drug delivery, and adaptive smart materials. However, the inherently non-equilibrium nature of active matter poses a significant challenge in achieving optimal control with minimal energy cost. In this work, we extend the concept of thermodynamic geometry, traditionally applied to passive systems, to active matter, proposing a systematic geometric framework for minimizing energy cost in non-equilibrium driving processes. We derive a cost metric that defines a Riemannian manifold for control parameters, enabling the use of powerful geometric tools to determine optimal control protocols. The geometric perspective reveals that, unlike in passive systems, minimizing energy cost in active systems involves a trade-off between intrinsic and external dissipation, leading to an optimal transportation speed that coincides with the self-propulsion speed of active matter. This insight enriches the broader concept of thermodynamic geometry. We demonstrate the application of this approach by optimizing the performance of an active monothermal engine within this geometric framework.

*Introduction.*—The thermodynamic control of active matter is an emerging field that integrates principles of non-equilibrium thermodynamics and statistical mechanics with the study of active systems [1]. Active matter refers to systems that continuously consume energy to generate self-sustained activity, leading to complex collective behaviors [2]. Understanding and controlling these systems from a thermodynamic perspective holds immense potential for a wide range of applications, including optimizing the performance of synthetic molecular motors to mimic biological functions [3, 4], designing low-energy drug delivery pathways to target specific sites [5–7], and developing smart materials that can dynamically adapt to external stimuli, like temperature, pressure, or electric fields [8, 9]. Achieving these tasks often requires the rapid steering of active matter toward a desired state. However, the inherently non-equilibrium nature of active matter introduces a complex interplay between external control and internal activity, complicating the prediction of the most efficient protocols for driving the system.

The quest for finding optimal control protocols with minimal energy cost in passive systems is a critical problem that has been thoroughly explored within the context of stochastic thermodynamics [10–13]. One of the most systematic approaches for addressing this is thermodynamic geometry, which transforms the challenge of designing an optimal control protocol into the problem of searching the geodesic path in a geometric space defined by control parameters [14–16]. As the controllable dimensions of the parametric space grow sufficiently expressive, thermodynamic geometry converges with optimal transport theory [17–20], which maps a source distribution to a target distribution with minimal entropy pro-

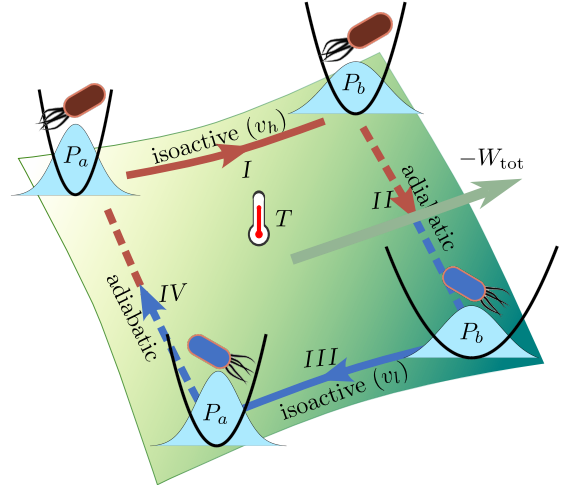


FIG. 1. Scheme for an active monothermal engine with performance optimized in a geometric space. The black curve represents a time-dependent control potential  $U(\mathbf{r}, t)$  applied to the active matter, while the filled blue curve indicates the boundary conditions  $P_a$  and  $P_b$  of the probability distribution  $P(\mathbf{r}, t)$ . Steps I and III correspond to isoactive processes with different activity levels,  $v_h$  and  $v_l$ , respectively. Steps II and IV are adiabatic processes where the activity switches instantaneously between  $v_h$  and  $v_l$ , while the system distribution holds unchanged. Throughout the cyclic process, the active matter remains in contact with a thermal bath at a constant temperature  $T$  to produce work  $-W_{\text{tot}}$ , which can be optimized using the geometric approach proposed in this work.

duction [21]. This geometric approach has been widely applied to various non-equilibrium systems, such as the Ising model [22, 23], bit initialization [24–26], and artificial thermal machines [27–29]. The success of this approach motivates us to extend it to the search for optimal control protocols beyond inherent passive systems.

\* tuzc@bnu.edu.cn

† gengli@bnu.edu.cn

However, how this geometric approach can be adapted to active matter remains an open question.

In this work, we propose a systematic geometric framework for determining the optimal control protocols with minimal energy cost in active systems. We demonstrate that the energy cost of thermodynamic control is governed by a positive cost metric, which can be minimized using optimal transport theory. When the controllable parameters are limited, this cost metric defines a Riemannian manifold spanned by the control parameters, and the optimal control protocol is obtained through the thermodynamic geometry scheme. In contrast to passive systems, where energy minimization leads to a vanishing transportation speed, we find that minimizing entropy production in active systems requires balancing intrinsic and external dissipation, suggesting the existence of a finite optimal transportation speed. The geometric viewpoint further shows that such an optimal transportation speed just corresponds to the self-propulsion speed of active matter. As shown in Fig. 1, we apply this framework to optimize the performance of an active monothermal engine, demonstrating the practicality of our approach in driving active matter systems.

*Theoretical model of active matter.*—Consider active matter immersed in a thermal bath at a constant temperature  $T$ , controlled by the potential  $U(\mathbf{r}, t)$ , where  $\mathbf{r} \equiv (r_1, r_2, r_3)$  represents the three-dimensional spatial coordinate. The motion of the active matter is governed by the Langevin equation:

$$\gamma \dot{\mathbf{r}} = -\nabla U + \boldsymbol{\xi} + \gamma v \mathbf{n}, \quad \dot{\mathbf{n}} = \boldsymbol{\chi} \times \mathbf{n}, \quad (1)$$

where  $v \mathbf{n}$  represents the self-propulsion velocity with a constant norm  $v$  and unit orientation vector  $\mathbf{n}$ . The terms  $\boldsymbol{\xi}$  and  $\boldsymbol{\chi}$  are uncorrelated Gaussian white noises with zero mean and variances  $\langle \xi_i(t) \xi_j(t') \rangle = 2\gamma T \delta_{ij} \delta(t - t')$  and  $\langle \chi_i(t) \chi_j(t') \rangle = 2(T/\gamma_r) \delta_{ij} \delta(t - t')$ , respectively. Here,  $\gamma$  and  $\gamma_r$  represent the translational and rotational friction coefficients. For simplicity, the Boltzmann constant  $k_B$  is set to unity. Considering a homogeneous active system, we average over the rotational degrees of freedom to obtain a theoretically tractable dynamical equation [30–32],

$$\gamma \dot{\mathbf{r}} = -\nabla U + \boldsymbol{\xi} + \boldsymbol{\eta}, \quad (2)$$

where  $\boldsymbol{\eta}$  is Gaussian colored noise with  $\langle \eta_i(t) \rangle = 0$  and  $\langle \eta_i(t) \eta_j(t') \rangle = (\gamma T D_a / \tau_p) \delta_{ij} e^{-|t-t'|/\tau_p}$ . Here,  $\tau_p \equiv \gamma_r / (2T)$  is the persistence time, and  $D_a \equiv \gamma v^2 \tau_p / (3T)$  is the activity parameter.

In a dilute suspension, where  $\tau_p$  is much shorter than the mean collision time, the evolution of the active matter's probability distribution  $P(\mathbf{r}, t)$  can be described using the Fokker-Planck equation:

$$\frac{\partial P(\mathbf{r}, t)}{\partial t} = -\nabla \cdot \mathbf{J}(\mathbf{r}, t) \quad (3)$$

with the probability current  $\mathbf{J}(\mathbf{r}, t) \equiv -(1/\gamma)[(\nabla U)P + T(1 + D_a)\nabla P]$ , keeping terms up to the first order in the

persistence time  $\tau_p$ . Detailed derivations of Eq. (3) are provided in Supplemental Material [33].

*Energy cost of thermodynamic control.*—The key challenge in controlling active matter lies in finding an optimal control protocol that minimizes the energy cost during a non-equilibrium process over a time interval  $[0, \tau]$ . The energy cost is quantified by the mean input work [34, 35]:

$$\begin{aligned} W &\equiv \int_0^\tau \langle \frac{\partial U}{\partial t} \rangle dt = \Delta \langle U \rangle - \int_0^\tau \langle \nabla U \circ \dot{\mathbf{r}} \rangle dt \\ &= \Delta \langle U \rangle - T(1 + D_a)\Delta S + \int_0^\tau dt \int d\mathbf{r} \frac{\gamma \mathbf{J}^2}{P}, \quad (4) \end{aligned}$$

where  $\langle \cdot \rangle$  denotes an ensemble average over stochastic trajectories with  $\Delta \langle U \rangle \equiv \langle U \rangle|_0^\tau$ , and the circle  $\circ$  between two stochastic variables represents Stratonovich calculus.  $S(t) \equiv -\int d\mathbf{r} P \ln P$  is the Gibbs entropy with  $\Delta S \equiv S(t)|_0^\tau$ . Please see Supplemental Material [33] for detailed derivations of Eq. (4). The first two terms in Eq. (4) are determined by the given initial and final probability distributions. Thus, the optimization focuses on the third term,  $\gamma \int_0^\tau dt \int d\mathbf{r} \mathbf{J}^2 / P$ , which defines a cost metric in the space of probability distributions [17–19]. The optimal scheme of transforming an active system from one probability distribution to another can be solved by using optimal transport theory. Interestingly, the irreversible part of the mean work for active matter is formally equivalent to that of a passive Brownian particle system [36].

Through a parametric design of the evolution path  $P(\mathbf{r}, t) = P(\mathbf{r}, \boldsymbol{\lambda}(t))$  connecting the initial and final states, the potential can be decomposed as  $U = U_o + U_a$ , where the original potential is defined as  $U_o(\mathbf{r}, \boldsymbol{\lambda}) \equiv -T(1 + D_a) \ln P(\mathbf{r}, \boldsymbol{\lambda})$ , and the auxiliary potential is  $U_a \equiv U - U_o$ . Here,  $\boldsymbol{\lambda}(t) \equiv (\lambda_1, \lambda_2, \dots, \lambda_M)$  represents various time-dependent control parameters. It has been shown that the auxiliary potential follows the form  $U_a = \boldsymbol{\lambda} \cdot \mathbf{f}(\mathbf{r}, \boldsymbol{\lambda})$ , where  $\mathbf{f}$  is determined by the evolution equation in Eq. (3) [33]. The irreversible part of the mean work  $W_o$  can then be expressed in a geometric form [33]:

$$\begin{aligned} W_o &\equiv W - \Delta \langle U \rangle + T(1 + D_a)\Delta S \\ &= \sum_{\mu\nu} \int_0^\tau dt \dot{\lambda}_\mu \dot{\lambda}_\nu g_{\mu\nu} \quad (5) \end{aligned}$$

where the positive semi-definite metric  $g_{\mu\nu} \equiv (1/\gamma) \sum_i \int (\partial f_\mu / \partial r_i) (\partial f_\nu / \partial r_i) P(\mathbf{r}, \boldsymbol{\lambda}) d\mathbf{r}$  induces a Riemannian manifold on the parametric space [16]. Thus, the challenge of minimizing energy cost in active systems can be reinterpreted as finding the geodesic path in the parametric space. This “thermodynamic geometry” scheme has been successfully applied to passive systems for solving optimal control protocols [14, 15, 37, 38]. Here, we extend this geometric framework to active matter, demonstrating its adaptability for optimizing thermodynamic control in persistently far-from-equilibrium conditions. This is our first main result.

*Optimal control duration.*—Based on the framework of stochastic thermodynamics [10, 39], we define the mean absorbed heat during the control of active matter as:

$$\begin{aligned} Q &\equiv \int_0^\tau \langle (-\gamma \dot{\mathbf{r}} + \boldsymbol{\xi}) \circ \dot{\mathbf{r}} \rangle dt = \int_0^\tau \langle (\nabla U - \boldsymbol{\eta}) \circ \dot{\mathbf{r}} \rangle dt \\ &= T\Delta S - \gamma v^2 \tau - \int_0^\tau dt \int d\mathbf{r} \left[ \frac{\gamma \mathbf{J}^2}{P} - \frac{T\tau_p v^2 (\nabla P)^2}{3P} \right], \end{aligned} \quad (6)$$

with the derivations of the third equality presented in Supplemental Material [33]. To facilitate comparison with passive systems, we rewrite Eq. (6) as a balance equation for the entropy production of active matter:

$$\begin{aligned} \Delta S_{\text{tot}} &\equiv \Delta S - \frac{Q}{T} \\ &= \frac{\gamma v^2 \tau}{T} + \int_0^\tau dt \int d\mathbf{r} \left[ \frac{\gamma \mathbf{J}^2}{TP} - \frac{\tau_p v^2 (\nabla P)^2}{3P} \right], \end{aligned} \quad (7)$$

which is always positive since the last term is a first order small quantity of  $\tau_p$ . The first term in Eq. (7) arises from sustained energy dissipation to maintain the activity, which increases linearly with the control duration  $\tau$ . The second term represents entropy production due to the non-equilibrium control, which takes the same form as in passive systems [36]. Unlike in passive systems, the results in Eq. (7) can be treated as a modified second law of thermodynamics in active systems.

When considering an optimal control protocol, solved using either optimal transport theory [19] or the thermodynamic geometry scheme [16], we obtain the scaling relations  $P(\mathbf{r}, t) = \mathcal{P}(\mathbf{r}, s)$  and  $\mathbf{J}(\mathbf{r}, t) = \mathcal{J}(\mathbf{r}, s)/\tau$  with normalized time  $s \equiv t/\tau$ , as proven in Supplemental Material [33]. The entropy production in Eq. (7) can then be rewritten as a scaling relation:

$$\begin{aligned} \Delta S_{\text{tot}} &= \frac{\gamma v^2 \tau}{T} + \int_0^1 ds \int d\mathbf{r} \left[ \frac{\gamma \mathcal{J}^2}{T\mathcal{P}\tau} - \frac{\tau_p v^2 (\nabla \mathcal{P})^2 \tau}{3P} \right] \\ &= \frac{E_a}{T} \tau + \frac{A_o}{T} \frac{1}{\tau}, \end{aligned} \quad (8)$$

where  $E_a \equiv \gamma v^2 [1 - \tau_p \int_0^1 ds \int d\mathbf{r} T (\nabla \mathcal{P})^2 / (3\gamma \mathcal{P})]$  and  $A_o \equiv \gamma \int_0^1 ds \int d\mathbf{r} \mathcal{J}^2 / \mathcal{P}$ . The first term in the second line of Eq. (8) reveals that the non-equilibrium dissipation from the activity accumulates linearly with the control time. The second term indicates that the irreversible energy cost of the optimal control follows a  $1/\tau$  scaling, a behavior widely discussed in passive systems [40–44]. The observation in Eq. (8) aligns with the results obtained by Davis *et al.*, who found a similar scaling relation for the optimal control of active systems in the slow and weak driving limit [45]. Here we demonstrate that this scaling relation applies to optimal thermodynamic control of active systems with arbitrary driving rates. This is our second major result.

This scaling relation implies an optimal control duration  $\tau^* = \sqrt{A_o/E_a}$  for achieving minimum entropy

production,  $\Delta S_{\text{tot}}^{\text{min}} = (2/T)\sqrt{A_o E_a}$ , in an active system. This contrasts with the monotonically decreasing relationship between entropy production and control duration found in passive systems. In the geometric space, the minimum  $A_o$  can be expressed as the square of the Wasserstein distance [17],  $\min A_o = \gamma \mathcal{W}^2$ , where the Wasserstein distance is defined as  $\mathcal{W} \equiv \int_0^1 ds \sqrt{\int d\mathbf{r} \mathcal{J}^2 / \mathcal{P}}$  describing the shortest distance between the initial and final states. The optimal control duration with minimum entropy production follows as  $\tau^* = \mathcal{W} / [v \sqrt{1 - \tau_p \int_0^1 ds \int d\mathbf{r} T (\nabla \mathcal{P})^2 / (3\gamma \mathcal{P})}]$ . Retaining terms up to the zero order in the persistence time  $\tau_p$ , we obtain that  $E_a \approx \gamma v^2$  and  $A_o \approx \gamma \int_0^1 ds \int d\mathbf{r} \mathcal{J}_0^2 / \mathcal{P}$ , where  $\mathcal{J}_0(\mathbf{r}, t) \equiv -(1/\gamma)[(\nabla U)\mathcal{P} + T\nabla \mathcal{P}]$ . The minimum entropy production is determined by the Wasserstein distance  $\mathcal{W} \approx \int_0^1 ds \sqrt{\int d\mathbf{r} \mathcal{J}_0^2 / \mathcal{P}}$  with the optimal control duration obtained as  $\tau^* = \mathcal{W}/v$ .

In passive systems, the geometric viewpoint suggests that the shortest path for transforming one state to another with minimum entropy production follows the geodesic line, whose length corresponds to the Wasserstein distance. The optimal transportation speed along the geodesic line is constant and approaches zero as we aim for minimum entropy production [17]. In sharp contrast, in active systems, the optimal transportation speed along the geodesic line has a finite value  $v$ , which happens to be the self-propulsion speed of the active system. When the speed is lower than  $v$ , dissipation from intrinsic activity dominates, whereas at speeds higher than  $v$ , energy cost from the external control becomes the dominant factor. These geometric perspectives lead to our third main result: our geometric framework not only provides a systematic approach for optimizing the thermodynamic control of active matter, but also imparts a clear geometric meaning to self-propulsion in active matter, enriching the broader concept of thermodynamic geometry.

*Active monothermal engines.*—As a practical application, we construct a cyclic engine operating with active matter to extract useful work and systematically investigate the optimization of its performance. As shown in Fig. 1, the active engine consists of two isoactive processes and two adiabatic processes with inverse boundary conditions  $P_a(\mathbf{r})$  and  $P_b(\mathbf{r})$ . Unlike passive thermal engines that operate between baths at different temperatures, the two isoactive processes in active engines operate within a single bath but with different self-propulsion speeds of active matter, where  $v_h > v_l$ . During the adiabatic process, the self-propulsion speed instantaneously changes between  $v_h$  and  $v_l$  while the system distribution keeps unaltered. Several experiments have confirmed the possibility of modulating the activity based on various physical or chemical factors [4, 46–49].

In a cyclic process, there is no net change in the potential energy or entropy of active systems, such that  $\sum_{i=1}^4 \Delta \langle U \rangle^{(i)} = \sum_{i=1}^4 \Delta S^{(i)} = 0$ . Since entropy remains constant during an adiabatic process, the entropy change

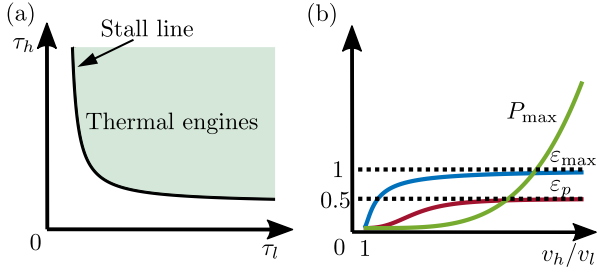


FIG. 2. Scheme for the performance of an active monothermal engine. (a) The stall line  $A_o/\tau_h + A_o/\tau_l = T(D_a^h - D_a^l)\Delta S$  for the active monothermal engine. Above this line, the cyclic process operates as a thermal engine, producing work. Below this line, the active cyclic process requires work input to function. (b) The maximum efficiency  $\epsilon_{\max}$  (blue curve), maximum power  $P_{\max}$  (green curve), and the efficiency at maximum power  $\epsilon_p$  (red curve) are shown as functions of the ratio between activity levels  $v_h/v_l$ . Here, the lower activity  $v_l$  is fixed. Both the maximum efficiency  $\epsilon_{\max}$ , maximum power  $P_{\max}$ , and the efficiency at maximum power  $\epsilon_p$  increase with the ratio  $v_h/v_l$ . As the ratio  $v_h/v_l$  grows,  $\epsilon_{\max}$  approaches 1, while  $\epsilon_p$  approaches 1/2.

in the isoactive process is  $\Delta S^{(1)} = -\Delta S^{(3)} \equiv \Delta S$ . By applying the optimal control protocol derived from the geometric approach to the isoactive process, the total output work and heat during a cycle follow as:

$$\begin{aligned} -W_{\text{tot}} &= T(D_a^h - D_a^l)\Delta S - \frac{A_o}{\tau_h} - \frac{A_o}{\tau_l}, \\ -Q_{\text{tot}} &= \frac{A_o}{\tau_h} + \frac{A_o}{\tau_l} + E_a^h\tau_h + E_a^l\tau_l, \end{aligned} \quad (9)$$

where  $D_a^h$  and  $D_a^l$  are the activity parameters,  $E_a^h$  and  $E_a^l$  are the scaling partial heat, and  $\tau_h$  and  $\tau_l$  denote the durations of the isoactive processes with self-propulsion speeds  $v_h$  and  $v_l$ , respectively. The scaling irreversible work  $A_o = \gamma\mathcal{W}^2$  is uniform for both isoactive processes due to the symmetry of the Wasserstein distance  $\mathcal{W}(P_a, P_b) = \mathcal{W}(P_b, P_a)$ .

The performance of the active monothermal engine can be evaluated by investigating the power and efficiency during a finite-time cycle. The efficiency  $\epsilon$  is defined as the ratio of the output work to the total energy cost [50–54]:

$$\begin{aligned} \epsilon &\equiv \frac{W_{\text{tot}}}{W_{\text{tot}} + Q_{\text{tot}}} \\ &= \frac{T(D_a^h - D_a^l)\Delta S - A_o/\tau_h - A_o/\tau_l}{T(D_a^h - D_a^l)\Delta S + E_a^h\tau_h + E_a^l\tau_l}, \end{aligned} \quad (10)$$

which is always less than one. As shown in Fig. 2(a), there exists a “stall line”  $A_o/\tau_h + A_o/\tau_l = T(D_a^h - D_a^l)\Delta S$ , where the engine stops producing work. Below this line, the engine starts consuming work. The maximum efficiency is given by  $\epsilon_{\max} = (\tau_h^*/\tau_h^e)^2 = (\tau_l^*/\tau_l^e)^2$ , where  $\tau_h^e$  and  $\tau_l^e$  represent the optimal driving durations for maximum efficiency, and  $\tau_h^* \equiv \sqrt{A_o/E_a^h}$  and  $\tau_l^* \equiv \sqrt{A_o/E_a^l}$

represent the optimal durations for minimum entropy production in the two isoactive processes. This behavior differs from that of passive thermal engines, which reach maximum efficiency at the long time limit. In Fig. 2(b),  $\epsilon_{\max}$  is plotted as a function of the activity ratio  $v_h/v_l$ . Here, the lower activity level  $v_l$  remains fixed while  $v_h/v_l$  is varied. As the activity ratio increases,  $\epsilon_{\max}$  rises and eventually approaches one. When  $v_h/v_l \rightarrow 1$ , the maximum efficiency scales as  $\epsilon_{\max} \propto (v_h/v_l - 1)^2$ , while at the large ratio limit  $v_h/v_l \rightarrow \infty$ , the maximum efficiency yields  $\epsilon_{\max} = 1 - \alpha v_h/v_l$ , where  $\alpha$  is a constant. Detailed expressions for  $\epsilon_{\max}$ ,  $\tau_h^e$ ,  $\tau_l^e$ ,  $\alpha$ , and the analytical relationship between  $\epsilon_{\max}$  and  $v_h/v_l$  are provided in Supplemental Material [33].

The power of the active engine  $P \equiv -W_{\text{tot}}/(\tau_h + \tau_l)$  reaches its maximum:

$$P_{\max} = \frac{T^2(D_a^h - D_a^l)^2(\Delta S)^2}{16A_o} \quad (11)$$

with optimal driving durations  $\tau_h^p = \tau_l^p = 4A_o/[T(D_a^h - D_a^l)\Delta S]$ . In Fig. 2(b), the maximum power  $P_{\max}$  is plotted as a function of the activity ratio  $v_h/v_l$ , following the analytical relationship  $P_{\max} \propto [(v_h/v_l)^2 - 1]^2$  [33]. The efficiency at maximum power is then obtained as

$$\begin{aligned} \epsilon_p &= \frac{1}{2\{1 + A_o(E_a^h + E_a^l)/[T^2(D_a^h - D_a^l)^2(\Delta S)^2]\}} \\ &= \frac{1}{2[1 + (E_a^h + E_a^l)/(16P_{\max})]}, \end{aligned} \quad (12)$$

which approaches 1/2 in the large ratio limit  $v_h/v_l \rightarrow \infty$ . The relationship between  $\epsilon_p$  and  $v_h/v_l$  is plotted in Fig. 2(b), with the analytical relation provided in Supplemental Material [33].

*Conclusions.*—In summary, we have proposed a geometric approach to optimize the thermodynamic control of active matter during finite-time state transitions. In a dilute suspension, the irreversible energy cost of active matter is characterized by a positive cost metric, defined on the space of probability distributions. Optimal control protocols are achieved by applying optimal transport theory. Considering the limited controllable parametric space, which is more practical for experiments and simulations, this cost metric describes a Riemannian manifold spanned by the control parameters, with the optimal control protocol corresponding to the geodesic path. Moreover, we have identified a trade-off between intrinsic and external dissipation when minimizing entropy production, revealing a constant optimal transportation speed along the geodesic line for non-equilibrium driving processes of active matter. The geometric perspective further suggests that the speed happens to be the self-propulsion speed of the active system, which endows the self-propulsion speed with a clear geometric significance. This behavior contrasts with passive systems, where the optimal transportation speed for minimum entropy production infinitely approaches zero. We have also demonstrated the practical utility of our approach by optimizing the performance of an active monothermal engine,

showing that both the maximum efficiency and maximum power monotonically increase with the activity ratio.

The geometric insights not only deepen our thermodynamic understanding of active matter's control, but also provide geometric interpretation of active matter's motion. The geometric framework establishes a direct link between the minimal-energy-cost path for active matter and the geodesic line in parametric space. Given a target state, optimal control protocols can be systematically obtained by solving the geodesic equation determined by the cost metric in Eq. (5), without the need to individually analyze complex active matter systems. It is intriguing to compare our theoretical findings on optimal control

of active matter, such as the scaling relation in Eq. (8), with biological evolution process in cells. Additionally, monothermal engines have been realized experimentally with a passive particle immersed in active bacterial baths [47]. It would be valuable to experimentally compare the performance of our active monothermal engine with that of the engine described in Ref. [47].

*Acknowledgement.*—This work is supported by the National Natural Science Foundation of China (NSFC) (Grants No. 12405031, No. 12475032, and No. 12305037) and the Fundamental Research Funds for the Central Universities (Grant No. 2233100001).

- 
- [1] E. Fodor, R. L. Jack, and M. E. Cates, *Annu. Rev. Condens. Matter Phys.* **13**, 215 (2022).
- [2] C. Bechinger, R. Di Leonardo, H. Löwen, C. Reichhardt, G. Volpe, and G. Volpe, *Rev. Mod. Phys.* **88**, 045006 (2016).
- [3] J. Palacci, S. Sacanna, A. P. Steinberg, D. J. Pine, and P. M. Chaikin, *Science* **339**, 936 (2013).
- [4] H. R. Vutukuri, M. Lisicki, E. Lauga, and J. Vermant, *Nat. Commun.* **11**, 2628 (2020).
- [5] N. Ahmad and Z. Mukhtar, *Genomics* **109**, 494 (2017).
- [6] S. Iram, E. Dolson, J. Chiel, J. Pelesko, N. Krishnan, Özenç Güngör, B. Kuznets-Speck, S. Deffner, E. Ilker, J. G. Scott, and M. Hinczewski, *Nat. Phys.* **17**, 135 (2020).
- [7] E. Ilker, Özenç Güngör, B. Kuznets-Speck, J. Chiel, S. Deffner, and M. Hinczewski, *Phys. Rev. X* **12**, 021048 (2022).
- [8] M. Bril, S. Fredrich, and N. A. Kurniawan, *Smart Materials in Medicine* **3**, 257 (2022).
- [9] M. Yildirim and Z. Candan, *Mater. Today: Proc.* **10**, 116 (2023).
- [10] U. Seifert, *Rep. Prog. Phys.* **75**, 126001 (2012).
- [11] S. Deffner and M. V. S. Bonança, *Europhys. Lett.* **131**, 20001 (2020).
- [12] D. Guéry-Odelin, A. Ruschhaupt, A. Kiely, E. Torrontegui, S. Martínez-Garaot, and J. Muga, *Rev. Mod. Phys.* **91**, 045001 (2019).
- [13] D. Guéry-Odelin, C. Jarzynski, C. A. Plata, A. Prados, and E. Trizac, *Rep. Prog. Phys.* **86**, 035902 (2023).
- [14] G. E. Crooks, *Phys. Rev. Lett.* **99**, 100602 (2007).
- [15] D. A. Sivak and G. E. Crooks, *Phys. Rev. Lett.* **108**, 190602 (2012).
- [16] G. Li, J.-F. Chen, C. P. Sun, and H. Dong, *Phys. Rev. Lett.* **128**, 230603 (2022).
- [17] J.-D. Benamou and Y. Brenier, *Numer. Math.* **84**, 375 (2000).
- [18] E. Aurell, C. Mejía-Monasterio, and P. Muratore-Ginanneschi, *Phys. Rev. Lett.* **106**, 250601 (2011).
- [19] A. Dechant and Y. Sakurai, arXiv:1912.08405 (2019), 10.48550/arXiv.1912.08405.
- [20] T. Van Vu and K. Saito, *Phys. Rev. X* **13**, 011013 (2023).
- [21] A. Zhong and M. R. DeWeese, *Phys. Rev. Lett.* **133**, 057102 (2024).
- [22] T. R. Gingrich, G. M. Rotskoff, G. E. Crooks, and P. L. Geissler, *Proc. Natl. Acad. Sci.* **113**, 10263 (2016).
- [23] M. D. Louwerse and D. A. Sivak, *J. Chem. Phys.* **156**, 194108 (2022).
- [24] Y.-H. Ma, J.-F. Chen, C. P. Sun, and H. Dong, *Phys. Rev. E* **106**, 034112 (2022).
- [25] A. B. Boyd, A. Patra, C. Jarzynski, and J. P. Crutchfield, *J. Stat. Phys.* **187**, 17 (2022).
- [26] G. Li and H. Dong, *Phys. Rev. E* **110**, 034115 (2024).
- [27] P. Abiuso, H. J. D. Miller, M. Perarnau-Llobet, and M. Scandi, *Entropy* **22**, 1076 (2020).
- [28] Z. Zhang, V. Du, and Z. Lu, *Phys. Rev. E* **107**, 1012102 (2023).
- [29] Z. Wang and J. Ren, *Phys. Rev. Lett.* **132**, 207101 (2024).
- [30] R. F. Fox, *Phys. Rev. A* **33**, 467 (1986).
- [31] Y. Fily and M. C. Marchetti, *Phys. Rev. Lett.* **108**, 235702 (2012).
- [32] T. F. F. Farage, P. Krinninger, and J. M. Brader, *Phys. Rev. E* **91**, 042310 (2015).
- [33] SupplementaryMaterials.
- [34] C. Jarzynski, *Phys. Rev. Lett.* **78**, 2690 (1997).
- [35] K. Sekimoto and S.-i. Sasa, *J. Phys. Soc. Jpn.* **66**, 3326 (1997).
- [36] U. Seifert, *Phys. Rev. Lett.* **95**, 040602 (2005).
- [37] P. Salamon and R. S. Berry, *Phys. Rev. Lett.* **51**, 1127 (1983).
- [38] G. Li, C. P. Sun, and H. Dong, *Phys. Rev. E* **107**, 014103 (2023).
- [39] K. Sekimoto, *Stochastic Energetics* (Springer-Verlag GmbH, 2010).
- [40] C. V. den Broeck, *Phys. Rev. Lett.* **95**, 190602 (2005).
- [41] T. Schmiedl and U. Seifert, *Europhys. Lett.* **81**, 20003 (2007).
- [42] M. Esposito, R. Kawai, K. Lindenberg, and C. V. den Broeck, *Phys. Rev. Lett.* **105**, 150603 (2010).
- [43] A. Ryabov and V. Holubec, *Phys. Rev. E* **93**, 050101 (2016).
- [44] Y.-H. Ma, R.-X. Zhai, J. Chen, C. Sun, and H. Dong, *Phys. Rev. Lett.* **125**, 210601 (2020).
- [45] L. K. Davis, K. Proesmans, and E. Fodor, *Phys. Rev. X* **14**, 011012 (2024).
- [46] I. Buttinoni, G. Volpe, F. Kümmel, G. Volpe, and C. Bechinger, *J. Phys. Condens. Matter* **24**, 284129 (2012).
- [47] S. Krishnamurthy, S. Ghosh, D. Chatterji, R. Ganapathy, and A. K. Sood, *Nat. Phys.* **12**, 1134 (2016).
- [48] A. Militaru, M. Innerbichler, M. Frimmer, F. Tebbenjo-

- hanns, L. Novotny, and C. Dellago, *Nat. Commun.* **12**, 2446 (2021).
- [49] M. Baldovin, D. Guéry-Odelin, and E. Trizac, *Phys. Rev. Lett.* **131**, 118302 (2023).
- [50] T. L. Hill, *Prog. Biophys. Mol. Biol.* **28**, 267 (1974).
- [51] F. Jülicher, A. Ajdari, and J. Prost, *Rev. Mod. Phys.* **69**, 1269 (1997).
- [52] P. Pietzonka, A. C. Barato, and U. Seifert, *J. Stat. Mech: Theory Exp.* **2016**, 124004 (2016).
- [53] G. Szamel, *Phys. Rev. E* **102**, 042605 (2020).
- [54] E. Fodor and M. E. Cates, *Europhys. Lett.* **134**, 10003 (2021).

# Supplementary Material: Thermodynamic Geometric Control of Active Matter

Yating Wang,<sup>1</sup> Enmai Lei,<sup>1</sup> Yu-Han Ma,<sup>1</sup> Z. C. Tu,<sup>1,\*</sup> and Geng Li<sup>2,†</sup>

<sup>1</sup>*School of Physics and Astronomy, Beijing Normal University, Beijing, 100875, China*

<sup>2</sup>*School of Systems Science, Beijing Normal University, Beijing 100875, China*

The supplementary materials are devoted to provide detailed derivations in the main context.

## CONTENTS

I. The Fokker-Planck equation for active matter	1
II. The mean input work done for active matter	2
III. The general form of the auxiliary potential	3
IV. The mean absorbed heat during the control of active matter	3
V. The optimal control of active matter	4
A. Optimal transport theory	5
B. The thermodynamic geometry scheme	6
VI. The performance of an active monothermal engine	6
A. The maximum efficiency	6
B. The maximum power	7
References	7

## I. THE FOKKER-PLANCK EQUATION FOR ACTIVE MATTER

The dynamics of a homogeneous active system is governed by a non-Markovian Langevin equation:

$$\gamma \dot{\mathbf{r}} = -\nabla U + \boldsymbol{\xi} + \boldsymbol{\eta}. \quad (1)$$

Applying the Fox approximation [1–3], the evolution equation for the probability distribution  $P(\mathbf{r}, t)$  is given by

$$\frac{\partial P(\mathbf{r}, t)}{\partial t} = -\nabla \cdot \mathbf{J}(\mathbf{r}, t), \quad (2)$$

where the probability current is:

$$\mathbf{J}(\mathbf{r}, t) \equiv -\frac{1}{\gamma} [(\nabla U(\mathbf{r}, t))P(\mathbf{r}, t) + T\nabla(\alpha(\mathbf{r}, t)P(\mathbf{r}, t))]. \quad (3)$$

The dimensionless parameter  $\alpha(\mathbf{r}, t)$  is defined as:

$$\alpha(\mathbf{r}, t) \equiv 1 + \frac{D_a}{1 + \frac{\tau_p}{\gamma} \nabla^2 U(\mathbf{r}, t)}. \quad (4)$$

In a dilute suspension, where the persistence time  $\tau_p$  is much smaller than the mean collision time, keeping terms up to the first order in  $\tau_p$ , the dimensionless parameter simplifies to  $\alpha \approx 1 + D_a$ . Therefore, the probability current reduces to:

$$\mathbf{J}(\mathbf{r}, t) \approx -\frac{1}{\gamma} [(\nabla U(\mathbf{r}, t))P(\mathbf{r}, t) + T(1 + D_a)\nabla P(\mathbf{r}, t)], \quad (5)$$

which is equivalent to the current in Eq. (3) of the main text. According to the probability current in Eq. (5), the equivalent Langevin equation becomes:

$$\gamma \dot{\mathbf{r}} = -\nabla U + \boldsymbol{\xi} + \boldsymbol{\xi}_a,$$

where  $\boldsymbol{\xi}_a$  represents Gaussian white noise with zero mean and variances  $\langle \xi_a^{(i)}(t) \xi_a^{(j)}(t') \rangle = 2\gamma T D_a \delta_{ij} \delta(t - t')$ .

## II. THE MEAN INPUT WORK DONE FOR ACTIVE MATTER

Based on the framework of stochastic thermodynamics [4, 5], the mean work performed in a non-equilibrium driving process is expressed as:

$$W \equiv \int_0^\tau \left\langle \frac{\partial U}{\partial t} \right\rangle dt = \Delta \langle U \rangle - \int_0^\tau \langle \nabla U \circ \dot{\mathbf{r}} \rangle dt, \quad (6)$$

where we have employed integration by parts. To evaluate the ensemble average in the second term, we apply a path integral formulation:

$$\begin{aligned} \langle \nabla U \circ \dot{\mathbf{r}} \rangle &= \int D[\mathbf{r}(t)] \mathcal{F}[\mathbf{r}(t)] \nabla U(\mathbf{r}(t), t) \circ \dot{\mathbf{r}}(t) \\ &= \frac{1}{\gamma} \int D[\mathbf{r}(t)] \mathcal{F}[\mathbf{r}(t)] \nabla U(\mathbf{r}(t), t) \circ [-\nabla U(\mathbf{r}(t), t) + \boldsymbol{\xi}(t) + \boldsymbol{\xi}_a(t)] \\ &= \frac{1}{\gamma} \int D[\mathbf{r}(t)] \mathcal{F}[\mathbf{r}(t)] \int d\mathbf{r} \delta(\mathbf{r} - \mathbf{r}(t)) \nabla U(\mathbf{r}(t), t) \circ [-\nabla U(\mathbf{r}(t), t) + \boldsymbol{\xi}(t) + \boldsymbol{\xi}_a(t)] \\ &= -\frac{1}{\gamma} \int d\mathbf{r} [\nabla U(\mathbf{r}, t)]^2 P(\mathbf{r}, t) + \frac{1}{\gamma} \int d\mathbf{r} \nabla U(\mathbf{r}, t) \circ [\langle \delta(\mathbf{r} - \mathbf{r}(t)) \boldsymbol{\xi}(t) \rangle + \langle \delta(\mathbf{r} - \mathbf{r}(t)) \boldsymbol{\xi}_a(t) \rangle]. \end{aligned} \quad (7)$$

In the fourth equality, we have employed the formulation  $P(\mathbf{r}, t) = \int D[\mathbf{r}(t)] \mathcal{F}[\mathbf{r}(t)] \delta(\mathbf{r} - \mathbf{r}(t))$ , where  $\mathcal{F}[\mathbf{r}(t)]$  represents the path probability. Considering the commutation between the noise terms  $\boldsymbol{\xi}(t)$  and  $\boldsymbol{\xi}_a(t)$  with the coordinate  $\mathbf{r}$  [6, 7], we derive:

$$\langle \delta(\mathbf{r} - \mathbf{r}(t)) \boldsymbol{\xi}(t) \rangle = -T \nabla P(\mathbf{r}, t) \quad (8)$$

and

$$\langle \delta(\mathbf{r} - \mathbf{r}(t)) \boldsymbol{\xi}_a(t) \rangle = -T D_a \nabla P(\mathbf{r}, t). \quad (9)$$

Substituting these into Eq. (7), we obtain:

$$\begin{aligned} \langle \nabla U \circ \dot{\mathbf{r}} \rangle &= -\frac{1}{\gamma} \int d\mathbf{r} \nabla U(\mathbf{r}, t) \circ [(\nabla U(\mathbf{r}, t)) P(\mathbf{r}, t) + T(1 + D_a) \nabla P(\mathbf{r}, t)] \\ &= \int d\mathbf{r} \nabla U(\mathbf{r}, t) \circ \mathbf{J}(\mathbf{r}, t) \\ &= - \int d\mathbf{r} \frac{\gamma \mathbf{J}(\mathbf{r}, t) + T(1 + D_a) \nabla P(\mathbf{r}, t)}{P(\mathbf{r}, t)} \circ \mathbf{J}(\mathbf{r}, t) \\ &= - \int d\mathbf{r} \frac{\gamma \mathbf{J}^2}{P} - T(1 + D_a) \int d\mathbf{r} \frac{\nabla P \circ \mathbf{J}}{P}. \end{aligned} \quad (10)$$

In the third equality, we have used the definition of the probability current in Eq. (5). Considering the time derivative of the Gibbs entropy  $S(t) \equiv - \int d\mathbf{r} P \ln P$ , we find:

$$\begin{aligned} \dot{S}(t) &= - \int d\mathbf{r} \frac{\partial P}{\partial t} \ln P \\ &= \int d\mathbf{r} \nabla \cdot \mathbf{J}(\mathbf{r}, t) \ln P \\ &= - \int d\mathbf{r} \frac{\nabla P \circ \mathbf{J}}{P} \end{aligned} \quad (11)$$

By leveraging the relations in Eqs. (10) and (11), we ultimately derive the mean work as:

$$W = \Delta \langle U \rangle - T(1 + D_a) \Delta S + \int_0^\tau dt \int d\mathbf{r} \frac{\gamma \mathbf{J}^2}{P}, \quad (12)$$

which is equivalent to the form in Eq. (4) of the main text.



### III. THE GENERAL FORM OF THE AUXILIARY POTENTIAL

Given the initial and final states, we can design an evolution path  $P(\mathbf{r}, t) = P(\mathbf{r}, \boldsymbol{\lambda}(t))$  with the time-dependent control parameters  $\boldsymbol{\lambda}(t) \equiv (\lambda_1, \lambda_2, \dots, \lambda_M)$ . With this setting, we split the potential  $U(\mathbf{r}, t)$  as  $U = U_o + U_a$  with the original potential defined as  $U_o(\mathbf{r}, \boldsymbol{\lambda}) \equiv -T(1 + D_a) \ln P(\mathbf{r}, \boldsymbol{\lambda}) + F(\boldsymbol{\lambda})$ . Here,  $F(\boldsymbol{\lambda})$  represents a normalization constant. Substituting this splitting into Eq. (2), we get

$$\dot{\boldsymbol{\lambda}}(\nabla_{\boldsymbol{\lambda}} F - \nabla_{\boldsymbol{\lambda}} U_o) = \frac{T(1 + D_a)}{\gamma} \nabla^2 U_a - \frac{1}{\gamma} \nabla U_o \nabla U_a. \quad (13)$$

By comparing both sides of Eq. (13), we arrive at the general form of the auxiliary potential:

$$U_a(\mathbf{r}, t) = \dot{\boldsymbol{\lambda}} \cdot \mathbf{f}(\mathbf{r}, \boldsymbol{\lambda}), \quad (14)$$

where the function  $\mathbf{f}(\mathbf{r}, \boldsymbol{\lambda})$  is determined by the evolution equation:

$$\nabla_{\boldsymbol{\lambda}} F - \nabla_{\boldsymbol{\lambda}} U_o = \frac{T(1 + D_a)}{\gamma} \nabla^2 \cdot \mathbf{f} - \frac{1}{\gamma} \nabla U_o \nabla \cdot \mathbf{f}. \quad (15)$$

With the general form of the auxiliary potential in Eq. (14), the irreversible part of the mean work can be rewritten as:

$$\begin{aligned} W_o &\equiv W - \Delta \langle U \rangle + T(1 + D_a) \Delta S \\ &= \int_0^\tau dt \int d\mathbf{r} \frac{\gamma \mathbf{J}^2}{P} \\ &= \frac{1}{\gamma} \sum_{\mu\nu} \int_0^\tau dt \dot{\lambda}_\mu \dot{\lambda}_\nu \sum_i \int (\partial f_\mu / \partial r_i) (\partial f_\nu / \partial r_i) P(\mathbf{r}, \boldsymbol{\lambda}) d\mathbf{r} \\ &= \sum_{\mu\nu} \int_0^\tau dt \dot{\lambda}_\mu \dot{\lambda}_\nu g_{\mu\nu} \end{aligned} \quad (16)$$

with the positive semi-definite metric  $g_{\mu\nu} \equiv (1/\gamma) \sum_i \int (\partial f_\mu / \partial r_i) (\partial f_\nu / \partial r_i) P(\mathbf{r}, \boldsymbol{\lambda}) d\mathbf{r}$ , representing a geometric space spanned by control parameters. The result in Eq. (16) is equivalent to the geometric expression in Eq. (5) of the main text.

### IV. THE MEAN ABSORBED HEAT DURING THE CONTROL OF ACTIVE MATTER

The mean heat absorbed during non-equilibrium control of active matter is expressed as:

$$\begin{aligned} Q &\equiv \int_0^\tau \langle (-\gamma \dot{\mathbf{r}} + \boldsymbol{\xi}) \circ \dot{\mathbf{r}} \rangle dt = \int_0^\tau \langle (\nabla U(\mathbf{r}(t), t) - \boldsymbol{\xi}_a) \circ \dot{\mathbf{r}} \rangle dt \\ &= \int_0^\tau \langle \nabla U(\mathbf{r}(t), t) \circ \dot{\mathbf{r}} \rangle dt - \int_0^\tau \langle \boldsymbol{\xi}_a \circ \dot{\mathbf{r}} \rangle dt. \end{aligned} \quad (17)$$

The first term is derived in Eq. (10), while the second term:

$$\begin{aligned}
\int_0^\tau \langle \boldsymbol{\xi}_a \circ \dot{\mathbf{r}} \rangle dt &= \int_0^\tau dt \langle \boldsymbol{\xi}_a(t) \circ \frac{1}{\gamma} (-\nabla U(\mathbf{r}(t), t) + \boldsymbol{\xi}(t) + \boldsymbol{\xi}_a(t)) \rangle \\
&= \frac{1}{\gamma} \int_0^\tau dt [-\langle \boldsymbol{\xi}_a(t) \circ \nabla U(\mathbf{r}(t), t) \rangle + \langle \boldsymbol{\xi}_a(t) \circ \boldsymbol{\xi}(t) \rangle + \langle \boldsymbol{\xi}_a(t) \circ \boldsymbol{\xi}_a(t) \rangle] \\
&= -\frac{1}{\gamma} \int_0^\tau dt \int d\mathbf{r} \nabla U(\mathbf{r}, t) \circ \langle \delta(\mathbf{r} - \mathbf{r}(t)) \boldsymbol{\xi}_a(t) \rangle + \frac{1}{\gamma} \frac{3\gamma T D_a \tau}{\tau_p} \\
&= -\frac{1}{\gamma} \int_0^\tau dt \int d\mathbf{r} \nabla U(\mathbf{r}, t) \circ (-T D_a \nabla P(\mathbf{r}, t)) + \frac{3T D_a \tau}{\tau_p} \\
&= \frac{T D_a}{\gamma} \int_0^\tau dt \int d\mathbf{r} \nabla U(\mathbf{r}, t) \circ \nabla P(\mathbf{r}, t) + \frac{3T D_a \tau}{\tau_p} \\
&= -\frac{T D_a}{\gamma} \int_0^\tau dt \int d\mathbf{r} \frac{\gamma \mathbf{J}(\mathbf{r}, t) + T(1 + D_a) \nabla P(\mathbf{r}, t)}{P(\mathbf{r}, t)} \circ \nabla P(\mathbf{r}, t) + \frac{3T D_a \tau}{\tau_p} \\
&= -T D_a \int_0^\tau dt \int d\mathbf{r} \frac{\nabla P \circ \mathbf{J}}{P} - \frac{T^2 D_a}{\gamma} \int_0^\tau dt \int d\mathbf{r} \frac{(\nabla P)^2}{P} + \frac{3T D_a \tau}{\tau_p} \\
&= T D_a \Delta S - \frac{T^2 D_a}{\gamma} \int_0^\tau dt \int d\mathbf{r} \frac{(\nabla P)^2}{P} + \frac{3T D_a \tau}{\tau_p}, \tag{18}
\end{aligned}$$

where we have neglected the second order of  $\tau_p$  in the seventh equality. In the second equality, we have the following considerations: The property of the colored noise  $\boldsymbol{\eta}(t)$  indicates that

$$\begin{aligned}
\langle \eta_i(t) \eta_j(t') \rangle &= \frac{\gamma T D_a}{\tau_p} \delta_{ij} e^{-|t-t'|/\tau_p} \\
&\stackrel{\tau_p \rightarrow 0}{=} 2\gamma T D_a \delta_{ij} \delta(t-t'). \tag{19}
\end{aligned}$$

However, when we consider the condition  $t = t'$ , the variance becomes

$$\langle \eta_i(t) \eta_j(t) \rangle = \frac{\gamma T D_a}{\tau_p} \delta_{ij} = \frac{\gamma^2 v^2}{3} \delta_{ij} \tag{20}$$

which holds as  $\tau_p \rightarrow 0$ . In the three-dimensional space, we have

$$\langle \boldsymbol{\eta}(t) \circ \boldsymbol{\eta}(t) \rangle \stackrel{\tau_p \rightarrow 0}{=} \langle \boldsymbol{\xi}_a(t) \circ \boldsymbol{\xi}_a(t) \rangle = \frac{3\gamma T D_a}{\tau_p}. \tag{21}$$

By using the relations in Eqs. (10) and (18), we find the mean absorbed heat as:

$$Q = T \Delta S - \frac{3T D_a \tau}{\tau_p} - \gamma \int_0^\tau dt \int d\mathbf{r} \frac{\mathbf{J}^2}{P} + \frac{T^2 D_a}{\gamma} \int_0^\tau dt \int d\mathbf{r} \frac{(\nabla P)^2}{P}. \tag{22}$$

Considering the activity parameter  $D_a \equiv \gamma v^2 \tau_p / (3T)$  in Eq. (22), we finally obtain:

$$Q = T \Delta S - \gamma v^2 \tau - \int_0^\tau dt \int d\mathbf{r} \left[ \frac{\gamma \mathbf{J}^2}{P} - \frac{T \tau_p v^2 (\nabla P)^2}{3P} \right]. \tag{23}$$

This result is equivalent to Eq. (6) in the main text.

## V. THE OPTIMAL CONTROL OF ACTIVE MATTER

In this section, the optimization of the control protocols for active matter is derived using two approaches: optimal transport theory and the thermodynamic geometry scheme.

### A. Optimal transport theory

The primary objective is to minimize the irreversible part of the mean work,  $W_o = \int_0^\tau dt \int d\mathbf{r} \gamma \mathbf{J}^2 / P$ . To achieve this, the system must satisfy the constraint given by the Fokker-Planck equation:

$$\frac{\partial P(\mathbf{r}, t)}{\partial t} = -\nabla \cdot \mathbf{J}(\mathbf{r}, t) = -\nabla \cdot (\mathbf{u}(\mathbf{r}, t)P(\mathbf{r}, t)), \quad (24)$$

where  $\mathbf{u}(\mathbf{r}, t)$  is the current velocity, defined as:

$$\mathbf{u}(\mathbf{r}, t) \equiv \frac{\mathbf{J}(\mathbf{r}, t)}{P(\mathbf{r}, t)} = -\frac{1}{\gamma} [\nabla U(\mathbf{r}, t) + T(1 + D_a) \nabla \ln P(\mathbf{r}, t)]. \quad (25)$$

To optimize  $W_o$ , the Lagrangian multiplier method is used, incorporating the constraint in the Fokker-Planck equation [8]. The Lagrangian is expressed as:

$$\begin{aligned} \mathcal{L} &= \int_0^\tau dt \int d\mathbf{r} \left\{ \frac{\gamma(\mathbf{J}(\mathbf{r}, t))^2}{P(\mathbf{r}, t)} - 2\phi(\mathbf{r}, t) \left[ \frac{\partial P(\mathbf{r}, t)}{\partial t} + \nabla \cdot (\mathbf{u}(\mathbf{r}, t)P(\mathbf{r}, t)) \right] + 2\psi(\mathbf{r}, t) \left[ \mathbf{u}(\mathbf{r}, t) + \frac{1}{\gamma} \nabla U(\mathbf{r}, t) \right. \right. \\ &\quad \left. \left. + \frac{T(1 + D_a)}{\gamma} \nabla \ln P(\mathbf{r}, t) \right] \right\} \\ &= \int_0^\tau dt \int d\mathbf{r} \left\{ \gamma(\mathbf{u}(\mathbf{r}, t))^2 P(\mathbf{r}, t) - 2\phi(\mathbf{r}, t) \left[ \frac{\partial P(\mathbf{r}, t)}{\partial t} + \nabla \cdot (\mathbf{u}(\mathbf{r}, t)P(\mathbf{r}, t)) \right] + 2\psi(\mathbf{r}, t) \left[ \mathbf{u}(\mathbf{r}, t) + \frac{1}{\gamma} \nabla U(\mathbf{r}, t) \right. \right. \\ &\quad \left. \left. + \frac{T(1 + D_a)}{\gamma} \nabla \ln P(\mathbf{r}, t) \right] \right\}, \end{aligned} \quad (26)$$

where  $\phi(\mathbf{r}, t)$  and  $\psi(\mathbf{r}, t)$  represent two Lagrangian multipliers. By optimizing over  $\mathbf{u}(\mathbf{r}, t)$ ,  $P(\mathbf{r}, t)$ ,  $\phi(\mathbf{r}, t)$ ,  $\psi(\mathbf{r}, t)$ , and  $U(\mathbf{r}, t)$ , the following equations are derived:

$$\begin{aligned} \frac{\delta \mathcal{L}}{\delta \mathbf{u}} &= 2\gamma \mathbf{u}(\mathbf{r}, t)P(\mathbf{r}, t) + 2(\nabla \phi(\mathbf{r}, t))P(\mathbf{r}, t) + 2\psi(\mathbf{r}, t) = 0, \\ \frac{\delta \mathcal{L}}{\delta P} &= \gamma(\mathbf{u}(\mathbf{r}, t))^2 + 2\frac{\partial \phi(\mathbf{r}, t)}{\partial t} + 2(\nabla \phi(\mathbf{r}, t))\mathbf{u}(\mathbf{r}, t) - \frac{2T(1 + D_a)}{\gamma} \frac{\nabla \psi(\mathbf{r}, t)}{P(\mathbf{r}, t)} = 0, \\ \frac{\delta \mathcal{L}}{\delta \phi} &= \frac{\partial P(\mathbf{r}, t)}{\partial t} + \nabla \cdot (\mathbf{u}(\mathbf{r}, t)P(\mathbf{r}, t)) = 0, \\ \frac{\delta \mathcal{L}}{\delta \psi} &= \mathbf{u}(\mathbf{r}, t) + \frac{1}{\gamma} \nabla U(\mathbf{r}, t) + \frac{T(1 + D_a)}{\gamma} \nabla \ln P(\mathbf{r}, t) = 0, \\ \frac{\delta \mathcal{L}}{\delta U} &= -\frac{2}{\gamma} \nabla \psi(\mathbf{r}, t) = 0. \end{aligned} \quad (27)$$

These simplify into:

$$\psi(\mathbf{r}, t) = 0, \quad (28)$$

$$\mathbf{u}(\mathbf{r}, t) = -\frac{1}{\gamma} \nabla \phi(\mathbf{r}, t), \quad (29)$$

$$\nabla U(\mathbf{r}, t) = \nabla \phi(\mathbf{r}, t) - T(1 + D_a) \nabla \ln P(\mathbf{r}, t), \quad (30)$$

$$\frac{\partial P(\mathbf{r}, t)}{\partial t} = -\nabla \cdot (\mathbf{u}(\mathbf{r}, t)P(\mathbf{r}, t)), \quad (31)$$

$$\frac{\partial \phi(\mathbf{r}, t)}{\partial t} = \frac{1}{2\gamma} (\nabla \phi(\mathbf{r}, t))^2. \quad (32)$$

Normalizing time as  $s \equiv t/\tau$  in Eq. (32), we obtain the scaling relations  $\phi(\mathbf{r}, t) = \Phi(\mathbf{r}, s)/\tau$  and  $\mathbf{u}(\mathbf{r}, t) = \mathbf{u}(\mathbf{r}, s)/\tau$ , which lead to  $P(\mathbf{r}, t) = \mathcal{P}(\mathbf{r}, s)$  and  $\mathbf{J}(\mathbf{r}, t) = \mathcal{J}(\mathbf{r}, s)/\tau$ . These indicate that driven by the optimal control protocol solved from optimal transport theory, the irreversible part of the mean work follows a scaling relation as

$$\begin{aligned} W_o &= \int_0^\tau dt \int d\mathbf{r} \frac{\gamma(\mathbf{J}(\mathbf{r}, t))^2}{P(\mathbf{r}, t)} \\ &= \frac{1}{\tau} \int_0^1 ds \int d\mathbf{r} \frac{\gamma(\mathcal{J}(\mathbf{r}, s))^2}{\mathcal{P}(\mathbf{r}, s)}. \end{aligned} \quad (33)$$

Similarly, the entropy production induced by the optimal control follows the scaling relation:

$$\begin{aligned}
\Delta S_{\text{tot}} &= \frac{\gamma v^2 \tau}{T} + \int_0^\tau dt \int d\mathbf{r} \left[ \frac{\gamma \mathbf{J}^2}{TP} - \frac{\tau_p v^2 (\nabla P)^2}{3P} \right] \\
&= \frac{1}{\tau} \int_0^1 ds \int d\mathbf{r} \frac{\gamma (\mathcal{J}(\mathbf{r}, s))^2}{T\mathcal{P}(\mathbf{r}, s)} + \tau \frac{\gamma v^2}{T} \left[ 1 - \tau_p \int_0^1 ds \int d\mathbf{r} \frac{T(\nabla \mathcal{P}(\mathbf{r}, s))^2}{3\gamma \mathcal{P}(\mathbf{r}, s)} \right] \\
&= \frac{A_o}{T} \frac{1}{\tau} + \frac{E_a}{T} \tau,
\end{aligned} \tag{34}$$

where  $A_o \equiv \gamma \int_0^1 ds \int d\mathbf{r} \mathcal{J}^2 / \mathcal{P}$  and  $E_a \equiv \gamma v^2 [1 - \tau_p \int_0^1 ds \int d\mathbf{r} T(\nabla \mathcal{P})^2 / (3\gamma \mathcal{P})]$ . This result is equivalent to the one in Eq. (8) of the main text.

## B. The thermodynamic geometry scheme

In the framework of thermodynamic geometry, the irreversible part of the mean work is obtained in Eq. (16) as  $W_o = \sum_{\mu\nu} \int_0^\tau dt \dot{\lambda}_\mu \dot{\lambda}_\nu g_{\mu\nu}$ . The optimal control protocol is found by solving the geodesic equation:

$$\ddot{\lambda}_\mu + \sum_{\nu\kappa} \Gamma_{\nu\kappa}^\mu \dot{\lambda}_\nu \dot{\lambda}_\kappa = 0, \tag{35}$$

where the Christoffel symbol is defined as  $\Gamma_{\nu\kappa}^\mu \equiv (1/2) \sum_i (g^{-1})_{i\mu} (\partial_{\lambda_\nu} g_{i\kappa} + \partial_{\lambda_\nu} g_{i\kappa} - \partial_{\lambda_i} g_{\nu\kappa})$ . By normalizing time as  $s \equiv t/\tau$  in Eq. (35), we arrive at the scaling relation of the optimal control as  $\boldsymbol{\lambda}(t) = \boldsymbol{\lambda}(s)$ , which leads to  $P(\mathbf{r}, \boldsymbol{\lambda}(t)) = \mathcal{P}(\mathbf{r}, \boldsymbol{\lambda}(s))$  and  $\mathbf{J}(\mathbf{r}, t) = \mathcal{J}(\mathbf{r}, s)/\tau$ . These conclusions lead to the same scaling relations as obtained from the optimal transport theory, i.e., Eqs. (33) and (34).

# VI. THE PERFORMANCE OF AN ACTIVE MONOTHERMAL ENGINE

## A. The maximum efficiency

The efficiency of the active monothermal engine is defined as:

$$\varepsilon \equiv \frac{W_{\text{tot}}}{W_{\text{tot}} + Q_{\text{tot}}} = \frac{T(D_a^h - D_a^l)\Delta S - A_o/\tau_h - A_o/\tau_l}{T(D_a^h - D_a^l)\Delta S + E_a^h\tau_h + E_a^l\tau_l}. \tag{36}$$

The scaling irreversible work  $A_o = \gamma \mathcal{W}^2$  is uniform for both isoactive processes due to the symmetry of the Wasserstein distance  $\mathcal{W}(P_a, P_b) = \mathcal{W}(P_b, P_a)$ . To optimize this efficiency with respect to the control durations  $\tau_h$  and  $\tau_l$ , we derive the following equations:

$$\begin{aligned}
[T(D_a^h - D_a^l)\Delta S + E_a^h\tau_h + E_a^l\tau_l]A_o/\tau_h^2 &= [T(D_a^h - D_a^l)\Delta S - A_o/\tau_h - A_o/\tau_l]E_a^h, \\
[T(D_a^h - D_a^l)\Delta S + E_a^h\tau_h + E_a^l\tau_l]A_o/\tau_l^2 &= [T(D_a^h - D_a^l)\Delta S - A_o/\tau_h - A_o/\tau_l]E_a^l.
\end{aligned} \tag{37}$$

Solving these yields the optimal durations for the high activity stage and the low activity stage:

$$\begin{aligned}
\tau_h^e &= \frac{A_o(1 + \sqrt{E_a^l/E_a^h})}{T(D_a^h - D_a^l)\Delta S} + \sqrt{\frac{A_o^2(1 + \sqrt{E_a^l/E_a^h})^2}{T^2(D_a^h - D_a^l)^2(\Delta S)^2} + \frac{A_o}{E_a^h}}, \\
\tau_l^e &= \frac{A_o(1 + \sqrt{E_a^h/E_a^l})}{T(D_a^h - D_a^l)\Delta S} + \sqrt{\frac{A_o^2(1 + \sqrt{E_a^h/E_a^l})^2}{T^2(D_a^h - D_a^l)^2(\Delta S)^2} + \frac{A_o}{E_a^l}}.
\end{aligned} \tag{38}$$

The maximum efficiency is then:

$$\varepsilon_{\text{max}} = \left(\frac{\tau_h^*}{\tau_h^e}\right)^2 = \left(\frac{\tau_l^*}{\tau_l^e}\right)^2, \tag{39}$$

where  $\tau_h^* \equiv \sqrt{A_o/E_a^h}$  and  $\tau_l^* \equiv \sqrt{A_o/E_a^l}$  represent the optimal driving durations for minimum entropy production in the two isoactive processes.

Comparing both sides of Eq. (32), we conclude that  $\phi(\mathbf{r}, t)$  is independent of the activity  $v$ , which leads to the independence of  $v$  for the optimal control of  $P(\mathbf{r}, t)$  and  $\mathbf{J}(\mathbf{r}, t)$ . Then, we finally derive that  $A_o \equiv \gamma \int_0^1 ds \int d\mathbf{r} \mathcal{J}^2 / \mathcal{P}$  is independent of  $v$  and  $E_a \equiv \gamma v^2 [1 - \tau_p \int_0^1 ds \int d\mathbf{r} T(\nabla \mathcal{P})^2 / (3\gamma \mathcal{P})] = F_a v^2$  is proportional to  $v^2$  with the function  $F_a$  independent of  $v$ . These results lead to

$$\begin{aligned} \frac{\tau_h^e}{\tau_h^*} = \frac{\tau_l^e}{\tau_l^*} &= \frac{\sqrt{A_o}(\sqrt{E_a^h} + \sqrt{E_a^l})}{T(D_a^h - D_a^l)\Delta S} + \sqrt{\frac{A_o(\sqrt{E_a^h} + \sqrt{E_a^l})^2}{T^2(D_a^h - D_a^l)^2(\Delta S)^2} + 1} \\ &= \frac{\sqrt{A_o}(\sqrt{F_a^h}v_h + \sqrt{F_a^l}v_l)}{(\gamma\tau_p\Delta S/3)(v_h^2 - v_l^2)} + \sqrt{\frac{A_o(\sqrt{F_a^h}v_h + \sqrt{F_a^l}v_l)^2}{(\gamma\tau_p\Delta S/3)^2(v_h^2 - v_l^2)^2} + 1}. \end{aligned} \quad (40)$$

By fixing the lower activity  $v_l$ , we obtain the function relationship between the maximum efficiency  $\varepsilon_{\max}$  and the ratio between activity levels  $v_h/v_l$ , which is drawn in Fig. 2(b) of the main text. In the limit  $v_h/v_l \rightarrow 1$ , the maximum efficiency satisfies the relation  $\varepsilon_{\max} = \alpha_1(v_h/v_l - 1)^2$  where  $\alpha_1 \equiv 4v_l^2\gamma^2\tau_p^2(\Delta S)^2/[9A_o(\sqrt{F_a^h} + \sqrt{F_a^l})^2]$ . While in the large ratio limit  $v_h/v_l \rightarrow \infty$ , the maximum efficiency yields  $\varepsilon_{\max} = 1 - \alpha_2 v_h/v_l$  where  $\alpha_2 = 9\sqrt{A_o F_a^h}/(v_l\gamma\tau_p\Delta S)$ .

## B. The maximum power

The power of the active monothermal engine follows as

$$P \equiv \frac{-W_{\text{tot}}}{\tau_h + \tau_l} = \frac{T(D_a^h - D_a^l)\Delta S - A_o/\tau_h - A_o/\tau_l}{\tau_h + \tau_l}. \quad (41)$$

By taking derivative over the durations  $\tau_h$  and  $\tau_l$ , we obtain:

$$\begin{aligned} 2A_o/\tau_h + A_o\tau_l/\tau_h^2 + A_o/\tau_l &= T(D_a^h - D_a^l)\Delta S, \\ 2A_o/\tau_l + A_o\tau_h/\tau_l^2 + A_o/\tau_h &= T(D_a^h - D_a^l)\Delta S. \end{aligned} \quad (42)$$

Solving these equations gives the durations for maximum power:

$$\tau_h^p = \tau_l^p = \frac{4A_o}{T(D_a^h - D_a^l)\Delta S}. \quad (43)$$

The maximum power is:

$$P_{\max} = \frac{T^2(D_a^h - D_a^l)^2(\Delta S)^2}{16A_o}, \quad (44)$$

which is proportional to  $[(v_h/v_l)^2 - 1]^2$  when the lower activity  $v_l$  is fixed. This result is represented in Fig. 2(b) of the main text. The efficiency at maximum power is then obtained as

$$\begin{aligned} \varepsilon_p &= \frac{1}{2\{1 + A_o(E_a^h + E_a^l)/[T^2(D_a^h - D_a^l)^2(\Delta S)^2]\}} \\ &= \frac{1}{2\{1 + A_o(F_a^h v_h^2 + F_a^l v_l^2)/[(\gamma\tau_p\Delta S/3)^2(v_h^2 - v_l^2)^2]\}}, \end{aligned} \quad (45)$$

which approaches 1/2 in the large ratio limit  $v_h/v_l \rightarrow \infty$ .

\* tuzc@bnu.edu.cn

† gengli@bnu.edu.cn

- [1] R. F. Fox, Phys. Rev. A **33**, 467 (1986).
- [2] R. F. Fox, Phys. Rev. A **34**, 4525 (1986).
- [3] T. F. F. Farage, P. Krinninger, and J. M. Brader, Phys. Rev. E **91**, 042310 (2015).
- [4] C. Jarzynski, Phys. Rev. Lett. **78**, 2690 (1997).
- [5] K. Sekimoto and S.-i. Sasa, J. Phys. Soc. Jpn. **66**, 3326 (1997).
- [6] L. E. Reichl, *A modern course in statistical physics* (Wiley, New York, 1998).
- [7] G. Li, J.-F. Chen, C. P. Sun, and H. Dong, Phys. Rev. Lett. **128**, 230603 (2022).
- [8] A. Dechant and Y. Sakurai, arXiv:1912.08405 (2019), 10.48550/arXiv.1912.08405.